Cladding Process Simulation And Residual Stress Estimation Using Finite Element Coupled Field Analysis

GK Purohit[1], Kalakesh Baligar[2]

[1]Professor, Mechanical Engineering Department, PDA College of Engineering, Gulbarga, Karnataka, India
[2]MTech (Production Engineering) Student, PDA College of Engineering, Gulbarga, Karnataka, India

Abstract

Material properties like hardness, yield strength, corrosion resistance, conduction properties plays important role in structural design and product life cycle. It is difficult to get a material with all required properties. So cladding is done to improve the required properties on the surface of the base metal. A number of experimental methods are there to determine the residual stresses produced during welding. However, a Finite element analysis is found to yield better approximations and also to analyze the thermo structural behavior of cladding process. Hence, in the present work an attempt is made to employ the Finite Element Analysis for the same. SA508 material is considered as the base material and cladding materials are changed to predict the nature of residual stresses. Element birth and death feature of ANSYS software is used to simulate the cladding process. Initially the geometry is built using top down approach of ANSYS. The geometry is split to ease the brick meshing of the geometry. With the appropriate elements, initially thermal analysis is carried out to find temperature distribution during cladding process. Block by block cladding simulation is carried out. Finally the structure is cooled it its initial temperature (No load condition) and coupled field analysis is carried out to find the residual stress nature. The effects of thickness on nature of residual stresses are also analyzed. Further analysis is carried out with general clad materials (Aluminium, brass and Zirconium).
.

Keywords—ANSYS, Submerged Arc Welding, Strip Cladding, Residual Stresses, Finite Element Analysis.

1. Introduction

1.1 Introduction

Materials nowadays require multiple conflicting properties such as high hardness and ductility. Different properties however are often required at different locations on the products. Wear and corrosion resistance are only required at the surfaces of products for instance. Surfaces of materials are always in contact with their surrounding, resulting in degradations due to wear, erosion and corrosion. Surface modification aims at reducing such surface degeneration. Surface modification may involve the application of a coating, for instance by using chemical vapour deposition, plasma spraying and strip cladding. Surface modification can be applied to all kinds of products to increase performance, reduce costs, and modify the surface properties independent of the bulk material. This enables the realization of products with improved functionality, at reduced use of scarce and expensive materials.

1.2 Cladding:

Cladding is a process where one material covers another. Cladding supplies a combination of desired properties not found in any one metal. A base metal can be selected for cost or structural properties, and another metal added for surface protection or some special property such as electrical conductivity. Thickness of the cladding can be made much heavier and more durable than obtainable by electroplating.

1.2.1 Strip Cladding

A superior coating technique, which manifests a metallic bonding of substrate and coating, is the Strip cladding technique. Strip cladding has become an important surface modification technique in today's industry and continues to gain market. Strip cladding is not only applied for coating but also for repair and refurbishment as well as for rapid prototyping.
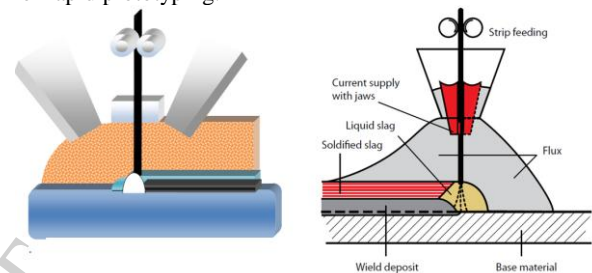

Fig. 1.1: Submerged Arc Strip Cladding

There are two types of Strip Cladding processes.
1) Submerged Arc Strip Cladding 2) Electro Slag Strip Cladding

Submerged Arc Strip Cladding utilizes an arc that runs back and forth at high speed along the strip, depositing weld metal onto the base material. Because this is an arc process there will be penetration into the base material resulting in dilution levels of 20%. Deposition rates are in the region of 10/12kg/hr for 60mm strip and are restricted by how much current can be applied.

Electro Slag Strip Cladding (ESW) utilizes a conductive flux and the resulting Joule heating effect to melt the strip into the liquid slag; which is transferred into molten metal deposited onto the base material. Higher current levels can be used giving deposition rates of 22-25kg/hr for 60mm strip.(SAW 10/12kg/hr). Utilizing high speed fluxes, dilution levels can be reduced and the area coverage (M2/hr) can be increased.

1.2.2 SAW cladding

SAW can be applied for joining and for overlay welding, i.e. depositing a corrosion resistant layer onto a mild (carbon) or low-alloyed steel. SAW produces coalescence of metals by heating them with an arc between a bare metal electrode and the work. The arc and molten metal are"submerged" in a blanket of granular fusible flux on the work piece. This flux plays a main role in that (i) the stability of the arc is dependent on the flux, (ii) mechanical and chemical properties of the final weld deposit can be controlled by the flux, and (iii) the quality of the weld may be affected by the care and handling of the flux. The flux also protects the welder from fumes and radiation, which raise environment advantages. The SAW process can only be used in a flat position (deviations of up to 6-8° may be

possible) since it would be difficult to retain the flux and steel melt in the inclined position. The wire (or strip) electrode is inserted into a mould of flux that covers the area or joint to be welded. An arc is initiated and a wire-feeding mechanism then begins to feed the electrode towards the joint at a controlled rate. Additional flux is continuously fed in front and around the electrode, and continuously distributed over the joint. Heat evolved by the electric arc progressively melts some of the flux, the end of the electrode, and the adjacent edges of the base metal, creating a pool of molten metal beneath a layer of molten slag. The melted slag bath near the arc is in a high turbulent state. Gas bubbles are quickly swept to the surface of the pool. As the welding zone progresses along the seam, the weld metal and then the liquid flux cool and solidify, forming a weld bead and a protective slag shield over it. Welding electrodes are supplied as solid wire, metal cored wire or strips. The electrodes can have a thin copper coating to provide good electrical contact, except those for welding corrosion resisting materials or for certain nuclear applications. Wire electrodes vary in size from 1.6 to 6 mm in diameter. The thickness of strips can vary between 0.5 to 1 mm and the width between 25 to 200 mm. A commonly used size is 60 x 0.5 mm. The main object of the flux is to protect the arc and weld pool from contamination with atmospheric oxygen and nitrogen. The flux should also provide arc stabilization properties, i.e. to facilitate ionization of the arc column. In addition the flux, when melted, should also provide slag of suitable viscosity and surface tension to ensure welds of good surface finish and shape.
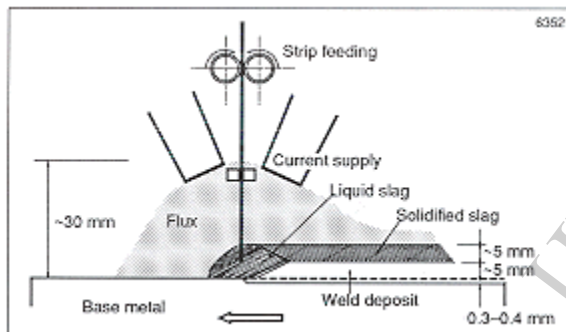

Fig. 1.2: Principle of SAW welding

Parameters of cladding quality:
a) Welding current

The strip cladding process is almost always performed with the positive polarity on the strip electrode (DCEP). With negative polarity, there is less penetration, and the weld bead tends to be thicker which could give steeper bead edges with increased risk for welding defects in the overlapping zones. The current transfer across the arc is not uniform across the width strip, as there is not one but a series of small arcs that wander across the end of the strip in the melting zone. A typical current density for SAW strip cladding is within the range 20 to 25A/mm^2. Increasing the current level will lead to a higher deposition rate but also the dilution will be higher.

b) Welding voltage

The optimum arc voltage to be used depends on different factors such as the welding flux, welding position and welding current. Increasing the voltage will lead to an increase in flux consumption.

c) Travelling speed

The welding travelling speed is generally related to the welding current being used and these two parameters are adjusted in tandem to give the desired combination of bead profile and bead thickness. Increasing the welding speed will lead to an increase of dilution.

Advantage of SAW
- High deposition rates(45kg/h) have been reported
- High operating factors in mechanized applications
- Deep weld penetration
- High speed welding of thin sheet steels upto 5m/mm is possible
- Minimal welding fume or arc light is emitted
- Distortion is much less
- Welds produced are sound, uniform, ductile and corrosion resistant and have good impact value
- 50 to 90% of flux is recoverable

Limitations of SAW:
- Limited to ferrous(steel or stainless steels) and some nickel based alloys
- Normally limited to long straight seams or rotated pipes or vessels.
- Requires relatively troublesome flux handling systems
- Flux and slag residue can present a health & safety concern.
- Requires inter-pass and post weld slag removal.

Applications of SAW:
- SAW is used for welding low carbon and medium carbon steel.
- For welding stainless steels, copper, aluminium and titanium base alloys
- SAW is also capable of welding heat resistant steels, corrosion resistant steels and high strength steels.
- SAW is widely used for butt and fillet welds in heavy industries like shipbuilding, pressure vessel fabrication, rail road tank cars, structural engineering, pipe welding and for storage tanks.
- Thinner material products such as water heaters and propane tanks.
- Hard facing for steel mills, earthmoving equipment, mining etc.

1.3   Cladding residual stresses

Because of significant difference in the thermal expansion coefficient between the austenitic cladding and the ferritic base metal, thermal stresses are induced in the cladding and the underlying base metal. Even after stress relieving and cooling down to room temperature, stresses of yield magnitude can be induced in the cladding and the cladding HAZ. The cladding residual stresses are temperature dependent, and decrease as the temperature increases. The magnitude and distribution of the cladding residual stresses depend on the temperature history during the cladding procedure, the geometry of the cladded component, the thickness of the cladding, the material properties of the base metal and the cladding, and the heat and pressure treatments both before and after the cladding process. These residual stresses are complex and often evaluated with the aid of experiments combined with computational modelling. Several destructive and non destructive methods are available for measurement of residual stresses; each having its advantages and disadvantages. Experimental evaluations are often based on laboratory tests conducted with specimens that are machined from cladded components. The experimental methods for determining the through-thickness residual stresses are based on relaxation technique and are destructive procedures, since they require cutting and machining of the plate. Deformations resulting from each cutting and machining step are monitored by surface strain gauges. These deformations are input data in a computational procedure which calculates the residual stresses that existed in the cladded plate before cutting. However, due to the differences in geometric stiffness (degree of restraint) in a laboratory small specimen and a real large structure, the experimental results from a

small specimen should be corrected to correspond to the real situations in the structure (reactor pressure vessel). This point has normally been ignored in the studies reported in the literature. Numerical evaluations of cladding residual stresses are often based on finite element analyses. However, there are many temperature dependent parameters which affect the magnitude and distribution of cladding residual stresses, and computational analyses are therefore normally performed under certain simplified assumptions.

2. Literature Survey

Literature survey on residual stresses:

A comprehensive literature search revealed a number of previous works on the subject of residual stress (R.S.) analysis. Heyn and Bauer [1], in their research on residual stresses in cold-drawn metals, illustrated the spring analogy to show how the residual stresses in metals behave. The amount of elongation experienced by the center springs is directly proportional to the force exerted on them by the outer springs. An exact method of determining the longitudinal, tangential, and radial residual stresses in bars or tubes was proposed by Mesnager [2] and modified by Sachs[3]. The method is limited to cylindrical bodies in which the residual stresses vary in the radial direction but are constant in the longitudinal and circumferential directions. The reaction of a material to externally applied stresses is influenced by the presence of residual stresses. On the other hand, compressive residual stresses will increase the yield stress. This principle first was employed in 1888 to manufacture built-up guns Hayes[4]. Timoshenko[5] presented a review of the early literature and theoretical treatment of manufactured parts such as guns and turbine rotors. Robertson[6] stated that residual stresses are as effective as stresses due to externally applied loads in producing stress corrosion cracking. A study was made by Demorest[7] of electro polishing methods of the residual stresses imposed upon copper strips subjected to various degrees of cold drawing and cold rolling. Analysis was made from the nature of the equilibrium distribution, which was determined experimentally by observing the curvature changes that occurred as thin layers of surface material were stripped. Horger[8] (1948) claimed that residual stresses in an elastic member would arise from three distinct sources namely misfit, change in specific volume, and non-uniform distortion. In a paper published by Leeser and Daane[9], the electro-polishing techniques were presented in a relatively simple and accurate way to determine residual stresses in a strip of rectangular cross section in terms of strain changes during electro-polishing. Dieter[10] stated that residual stresses cannot be determined directly from strain-gauge measurements, as is the case for stresses due to externally applied loads. Rather, residual stresses are calculated from the measurements of strain that are obtained when the body is sectioned and the locked-in residual stresses are released. Srinivasan, Hartley and Bandy[12] showed that electrochemical machining (ECM) provides a rapid, easily controlled and damage-free method of metal removal. P. Dupas[18] in his article "Evaluation of Cladding Residual Stresses in Clad Blocks by Measurements and Numerical Simulations" discussed about cladding process in the reactor vessels and measurement of residual stresses". According to these measurements, transversal stresses (perpendicular to the welding direction) and longitudinal stresses (parallel to the welding direction) are highly tensile in stainless steel and they are compressive in the HAZ. Finite element calculations were used to simulate both welding operations and post weld heat treatment. These calculations coupled the thermal, metallurgical and mechanical aspects in a 2D representation. Different models were studied including effect of generalized plane strain, transformation plasticity, creep and tempering.

The transversal stresses calculated are similar to the measured ones, but the longitudinal stresses showed to be very sensitive to the model used.

1.4.2. Literature Survey on Thermal Stresses

I. J. Kumar, D. Rajgopalan [11] presented Steady state thermal analysis and deformations in a hollow circular cylinder being head at the internal surface by a source which is sinusoidal along the length of the cylinder and with Newton type radiation boundary condition at the outer surface. The solution of the problem under given boundary condition has been obtained in the form of infinite integrals. G. Sánchez Sarmiento, M.J. Mizdrahi, P. Bastias and M. Pizzi [19] reviewed several finite element models for the determination of mechanical and thermal stresses in the SHS (Secondary Heat Sink) System. The models were developed by ABAQUS/CAE, solving with ABAQUS/Standard the problems of temperature distribution and of thermo-elastic-plastic stress and strain distribution of several components, subjected to complex loads of normal operation as well as postulated accidents. The design was based on internal pressure load, and further analysis take into account thermal shock, thermal stratification and pipe forces. Muhammad Abid [20] carried out analysis to investigate joint strength and sealing capability under combined internal pressure and different steady-state thermal loading, a 3D nonlinear finite element analysis (FEA) of a gasketed flange joint is carried out and its behaviour is discussed. They concluded that at higher temperatures the internal pressure must be lower for safe operating conditions.
M. Murali Krishna, M.S. Shunmugam and N. Siva Prasad [21] presented a three-dimensional finite element analysis (FEA) of bolted flange joints carried out by taking experimentally obtained loading and unloading characteristics of the gaskets. Experiments have been carried out for finding the loading and unloading characteristics of the gasket materials, which are in turn used in the FEA. The increase in the axial bolt force when the joint is subjected to an internal pressure has also been analyzed. Analysis shows that the distribution of contact stress has a more dominant effect on sealing performance than the limit on flange rotation specified by ASME. Mohammad A. Irfan and Walter Chapman [24] performed analysis of the thermal stresses in radiant tubes. The analytical analysis is verified using a finite element model. It was found that axial temperature gradients are not a source of thermal stresses as long as the temperature distribution is linear. Symmetric circumferential gradients generate thermal stresses, which are low as compared to the stress rupture value of radiant tubes. Radial temperature gradients create bi-axial stresses and can be a major source of thermal stress in radiant tubes. They concluded that the bends carry a higher stress level than the straight portion of the tube and a local hot spot generates stresses, which can lead to failure of the tube.

3. Problem Definition & Scope of the Work

3.1 Definition

"Evaluation of Residual Stresses in Clad Blocks and the base metal by Numerical Simulations is the main objective of the problem. So the problem objectives include:

- Finite element modelling of cladding process
- Finding temperature distribution across the base metal and clad metal
- Finding residual stresses in the cladding process
- Effect of thickness of cladding layer in residual stress formation
- Effect of material properties on residual stress formation
- Results presentation

3.2   Methodology

- Geometrical modelling of the clad material with the parent material using ANSYS top-down approach
- Brick-meshing of both parent and clad material
- Application of initial thermal boundary conditions
- Analysis for thermal results
- Coupled field analysis to find the residual stresses in the structure
- Representation of the graphical plots
- Results representation for variation in parameters
- Graphical plots for both temperature and stress across the thickness direction.
- Report generation

3.2.1   Flow chart for thermal analysis using ANSYS

ANSYS is a suite of powerful engineering simulation programs, based on the finite element method that can solve problems ranging from relatively simple linear analyses to the most challenging nonlinear simulations. ANSYS contains an extensive library of elements that can model virtually any geometry. Designed as a general-purpose simulation tool, ANSYS can be used to study more than just structural (stress/displacement) problems. It can simulate problems in such diverse areas as heat transfer, mass diffusion, thermal management of electrical components (coupled thermal-electrical analyses), acoustics, soil mechanics (coupled pore fluid-stress analyses), and piezoelectric analysis. In most simulations, including highly nonlinear ones, the user need only provide the engineering data such as the geometry of the structure, its material behavior, its boundary conditions, and the loads applied to it. In a nonlinear analysis ANSYS automatically chooses appropriate load increments and convergence tolerance.
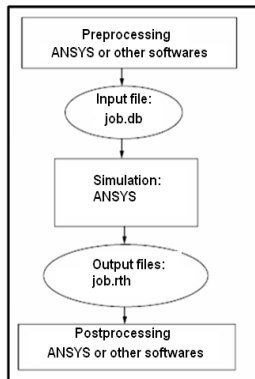
Fig. 3.1: Flow chart for ANSYS thermal analysis

3.2.2 ANSYS structural analysis from thermal results

Thermal results are taken to structural analysis as shown in the following block diagram (Fig. 3.2) for stress and deformation results.
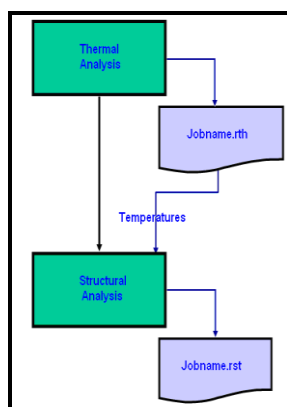

Fig. 3.2: Block Diagram of thermal structural analysis

The basic procedure for sequential coupled field thermal structural analysis is as given below.

- Define the thermal problem.
- Write the thermal file.
- Clear boundary conditions and options.
- Define the structural problem.
- Write the structural file.
- Read the thermal file.
- Solve and postprocessor the thermal problem.
- Read the structural file.
- Read the temperatures from the thermal results file.
- Solve and postprocessor the file.

3.3   Material Properties

Table 3.1: Material Properties

	Property	Value
Base Metal : Ferritic steel (SA508)	Young's Modulus	206GPa
	Poison's ratio	0.3
	Density	$7800Kg/m^3$
	Thermal Conductivity	$42w/m - K$
	Specific heat	365W
	Thermal expansion Coefficient	$11.7/^0c$
SA304	Young's Modulus	196GPa
	Poison's ratio	0.3
	Density	$7800Kg/m^3$
	Thermal Conductivity	$15w/m - K$
	Specific heat	465W
	Thermal expansion Coefficient	$18.7/^0c$

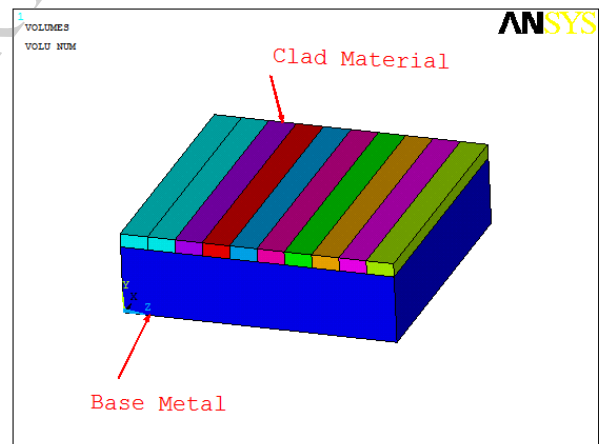## 3.4   Initial Geometrical Model:

Fig. 3.3: Geometrical Model of the problem

The figure 3.3 shows geometrical model of the base metal and clad material. The geometry is built using Ansys top down approach. The clad blocks are split and glued to the parent metal brick meshing. Ansys sweep mesher can brick mesh glued regular structures. Total 10 clad blocks are used for geometrical representation. 200mm length with 50mm depth is considered for the base metal. 20mm length by 10mm thickness is considered for the clad material. Due to dynamic nature of the structure the modelling is carried out in meters.
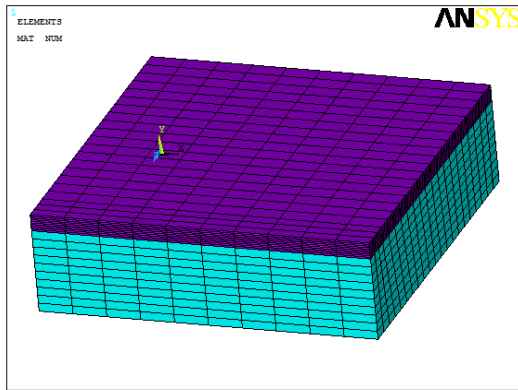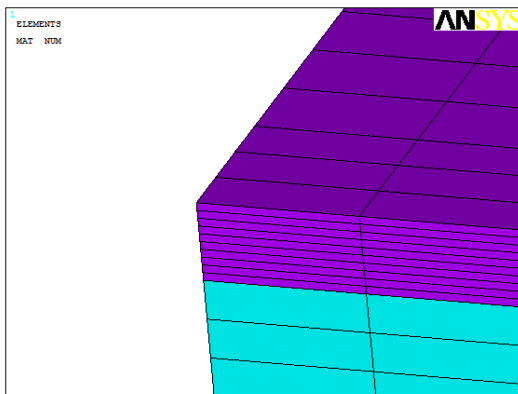
Fig. 3.4: Meshed Model

Fig. 3.5: Zoomed view of the Mesh

The figure shows brick mesh of both clad material and base material. Total numbers of elements are 4200 and numbers of nodes are 19393 nodes. Solid90 element properties are applied for the structure. For structural analysis, solid 95 element properties are applied on the process. Element birth and death property is used to simulate the process of cladding. The boundary conditions are changed as per the application of cladding process and continued till the complete process is done. Different colours show application of different material properties to the clad material and to the base metal. Initial complete geometry is meshed, but boundary conditions are applied only to the required geometry by killing unnecessary elements. Newton Raphson solver allows the execution of this type of problems.

The cladding region is fine meshed to obtain better results due to higher variation across the thickness of the structure and due to nearness of the metal to heat conditions. 10 elements are considered across the thickness of 4mm with 0.4mm size for the height along the height of the structure.

3.5 Element:
SOLID90 has a 3-D thermal conduction capability. The element has eight nodes with a single degree of freedom, temperature, at each node. The element is applicable to a 3-D, steady-state or transient thermal analysis. The element also can compensate for mass transport heat flow from a constant velocity field. If the model containing the conducting solid element is also to be analyzed structurally, the element should be replaced by an equivalent structural element
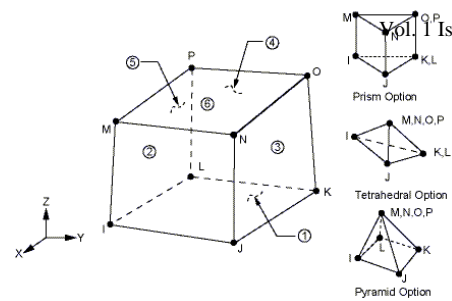
Fig. 3.6: Solid70 Element

3.6 Assumptions:
- The material is assumed to be in homogenous.
- 20 noded brick element is used for analysis
- All approximations applied to FEM are applicable for the analysis(FEM is approximate technique)
- ANSYS coupled field analysis used for structural and thermal results
- Residual stresses obtained after cooling it to room temperature

IV. RESULTS & DISCUSSION

Analysis has been carried out to find temperature distribution and residual stresses due to cladding by element birth and death feature. The bottom of the base material is insulated for thermal boundary conditions and convection loads are applied on the top. The initially the body is heated to $170\ ^0$c. The results are as follows.

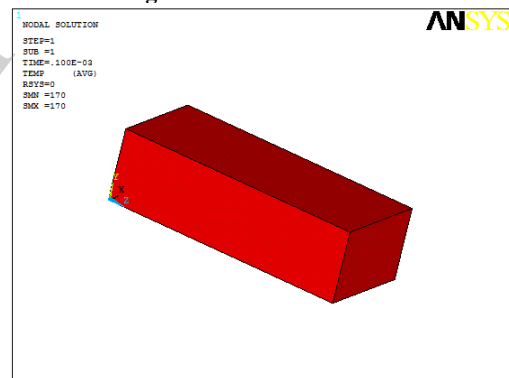**4.1 Cladding Simulation with Steel**

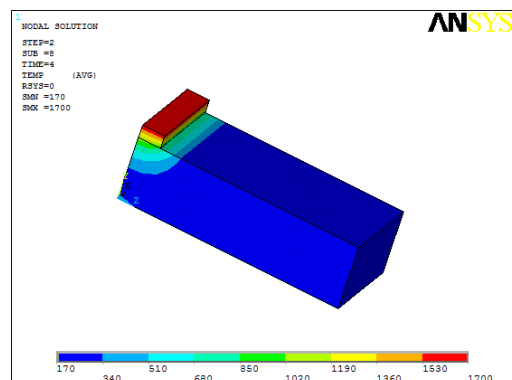**Fig. 4.1: Initial Condition of the problem**

Fig 4.2: Temperature distribution in the member

The figure 4.1 shows initial boundary conditions applied on the problem. A uniform temperature of 1700 is applied on the geometry. This was taken as the initial step for transient thermal analysis. Since no cladding process is started, no clad elements can be observed.

The figure 4.2 shows temperature distribution in the member. Maximum temperature is around 1700 and minimum is 170°C. By using element birth and death properties, elements which are subjected to cladding are made visible. Other elements are killed and hidden from the visibility. Maximum temperature can be observed at the top and reducing towards the base metal. At the base of base material, almost a temperature of 170°C can be observed. Away from the cladding region, the temperatures are minimum. A step size of 0.5 second is used to reduce the computational times.
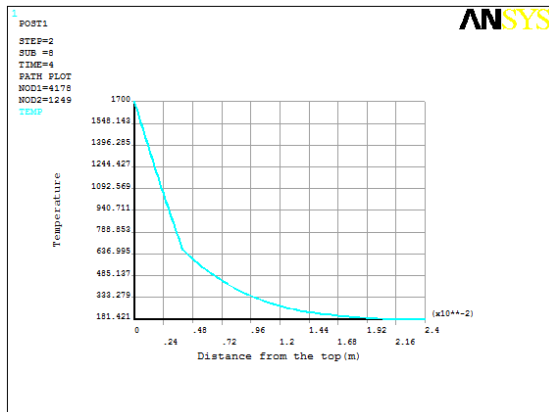
Fig. 4.3: Temperature across the thickness of the overall assembly
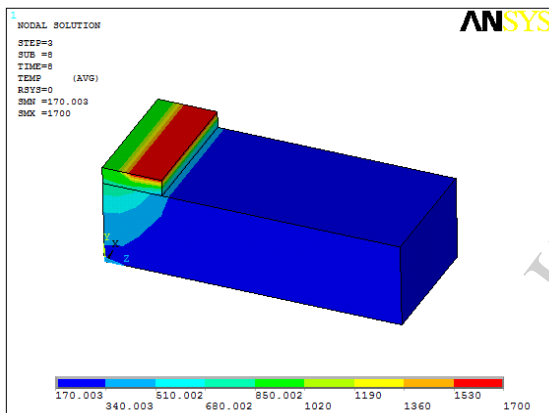
Fig. 4.4: Temperature distribution

The temperature is plotted from the top clad surface to the base material. The graph shows parabolic drop of temperature from top to bottom. Maximum temperatures are observed at the top and minimum at the base. The distance is represented in meters.

The figure shows temperature distribution in the member. Maximum temperature is around 1700°C and minimum is 170°C. By using element birth and death properties, elements which are subjected to cladding are made visible. Other elements are killed and hidden from the visibility. Now two clad blocks are visible and maximum temperature is observed at the present clad block and temperature is dropped at the previous clad block. The status bar at the bottom shows variation of temperature with colour code. Also not much heat is transferred
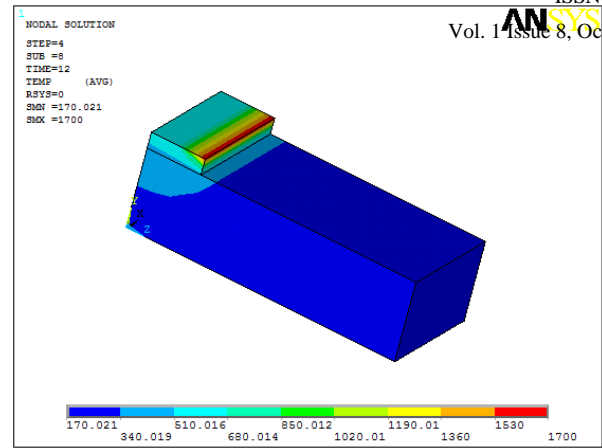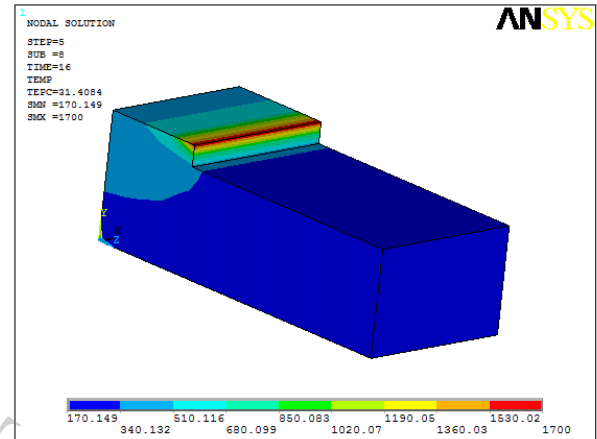

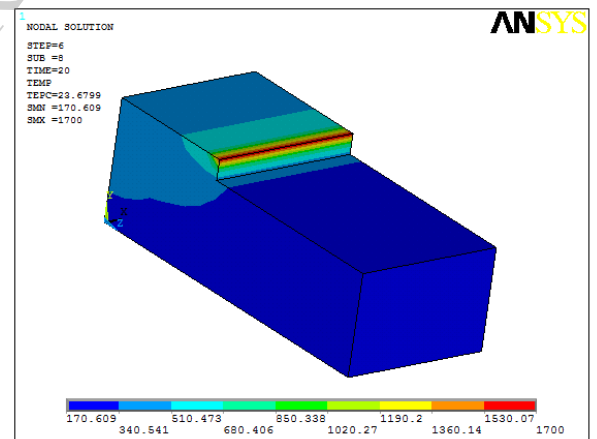**Fig. 4.5: Cladding at 3 block**

Fig. 4.6: Cladding at 4 block

Fig. 4.7: Cladding at 5 block

Fig. 4.8: Cladding at 6 block

Fig. 4.9: Cladding at 7 block

Fig. 4.10: Cladding at 8 block
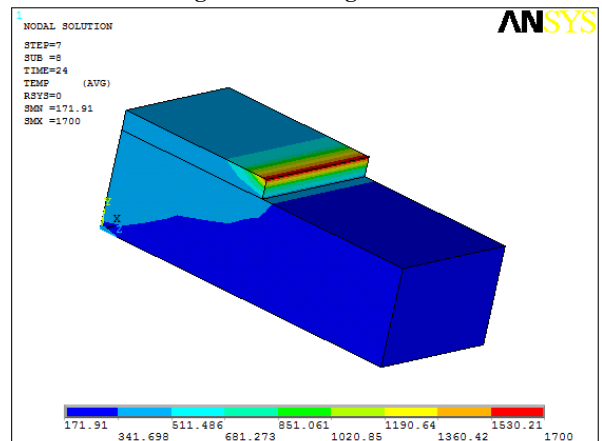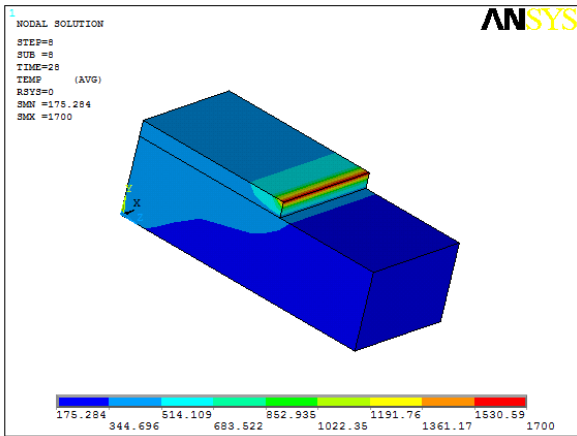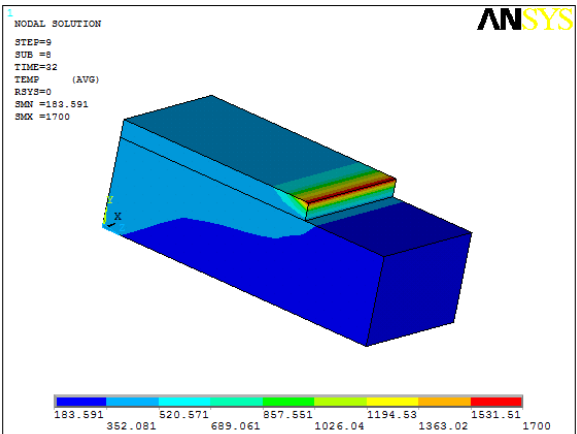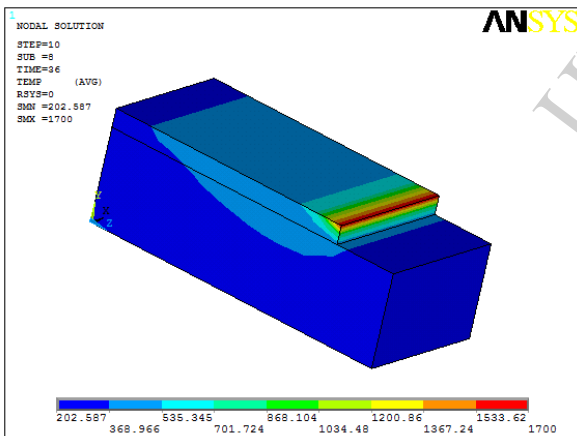

Fig. 4.11: Cladding at 9 block
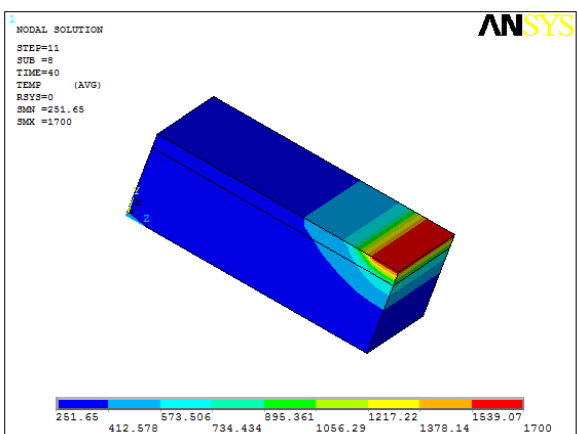
Fig. 4.12: Cladding at 10 block

The temperature distribution after one cycle of cladding is over. Minimum temperature of around 251.65 ^{0}c can be observed by the end of cladding process at the start of cladding. Maximum temperatures are concentrated around the cladding region. Totally 40 steps are considered with each time step of 4seconds with sub step size of 0.5 seconds.
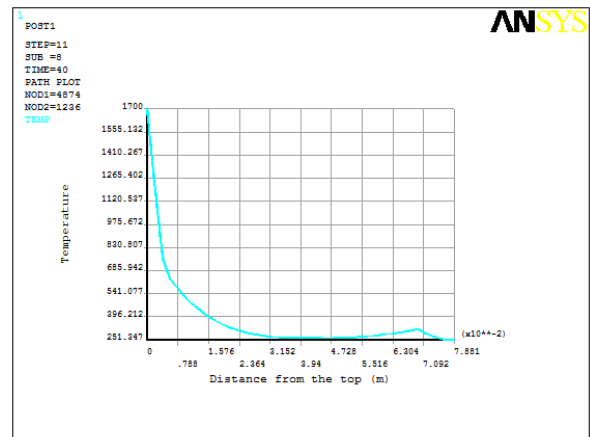

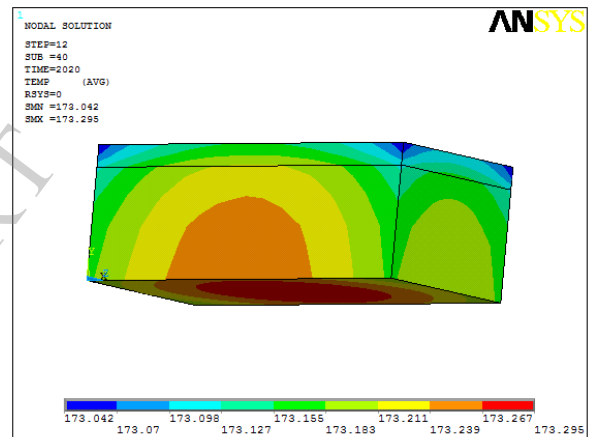**Fig. 4.13: Temperature variation the end of the cladding process**


Fig. 4.14: After 2000 seconds cooling

The graph shows variation of temperature across the clad region along the thickness direction. The drop of temperature is parabolic from top to bottom. Minimum temperatures are shows at the bottom and maximum at the top surface or cladding region. The X-axis is represented with distance measured in meters from top clad surface to bottom base metal.

The figure 4.14 shows temperature variation in the problem after cooling it for 2000 seconds to the base temperature. Maximum temperature can be observed at the base as this region is insulated from heat transfer. The temperatures in the other regions are represented with various colours.
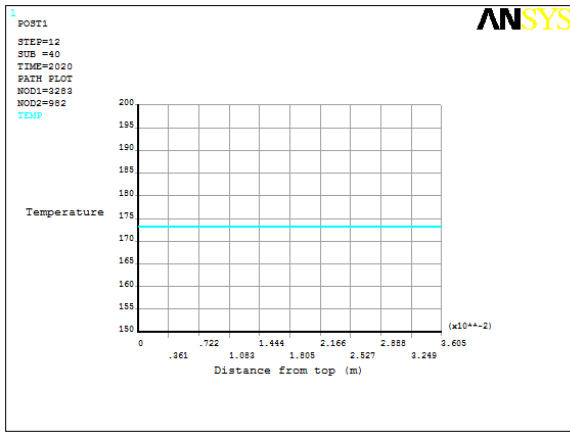
Fig. 4.15: After cooling temperature distribution in the structure

After cooling to the initial temperature, temperature plot is done to check the distribution. Almost, the same temperature can be observed across the geometry. Both clad material and base materials are brought to the initial temperature. At this point analysis is changed to Structural analysis from thermal loads. Bottom is constrained in all directions and thermal loads are taken from the thermal analysis to the corresponding nodes. The element type is switched from thermal element Solid90 to 20 noded structural element Solid95. The analysis is purely carried out only for thermal loads.
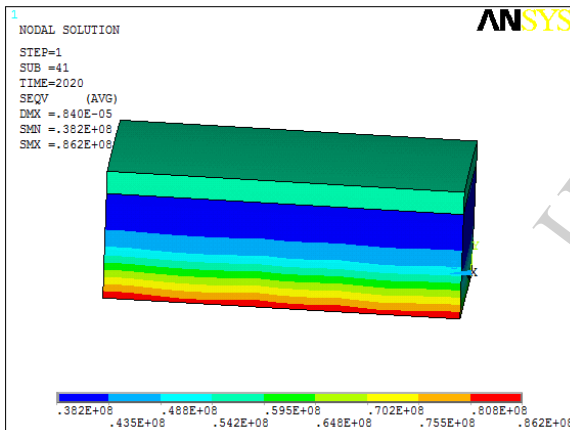

**Fig. 4.16: Overall Stress in the structure**
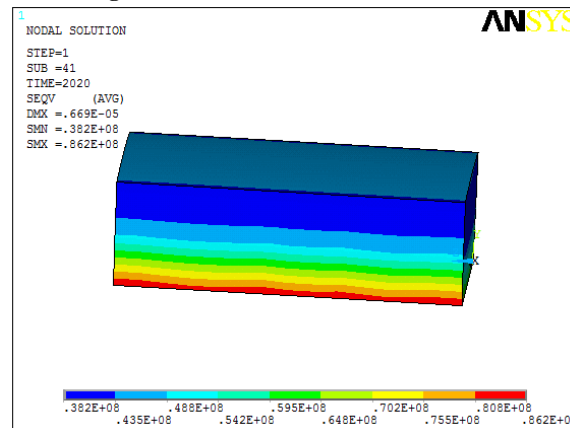
Fig 4.17: Base Metal Stress

The figure 4.16 shows vonmises stress in the structure. The bottom is observed more stress compared to the top region. Uniform stress variation can be observed from the top to the bottom geometry. Almost a stress of 38.2 Mpa can be observed at the interface between clad material and the base material. Also boundary conditions plays important role in the stress generation, as they allow free expansion which induce no stress in the structure.

The figure 4.17 shows stress generation in the base material. Minimum stress is observed on the top surface and maximum stress in the constrained region. This can be attributed to cantilever type arrangement due to higher deflection at the top which results in higher stress generation at the fixed ends.
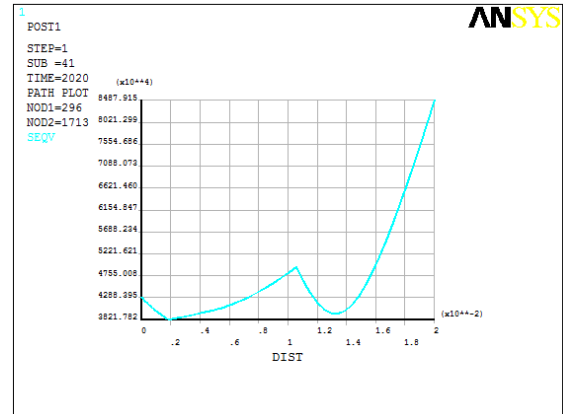
Fig 4.18: Stress in the Base Metal (from the top surface)
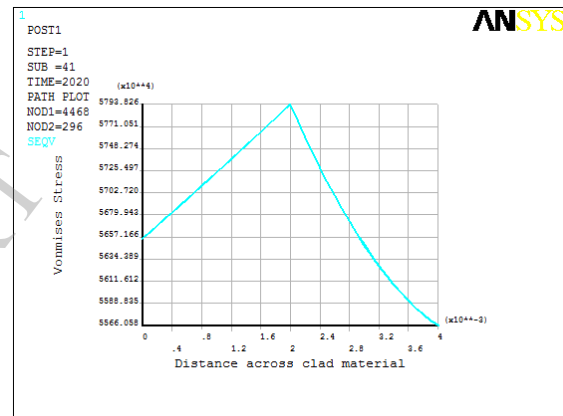
Fig. 4.19: Stress graph across the clad material

The figure 4.18 shows stress variation in the base material from top to the fixed end. Slightly higher stress can be observed at the interface and dropping to the initial depth. Later stress is increasing to the fixed region. Maximum stress is observed at the fixed region. A path is defined across the geometry from top to bottom of the structure by selecting the nodes and stress is mapped to obtain the graph.

The figure 4.19 shows residual stress generation in the clad material. Maximum stress observed at the center of the clad material. This can be attributed to differential expansion and distortion due to the material difference. Small variation can be observed between the stress at the top and stress at the bottom. The distance is measured in meters. To study the effect of clad layer thickness of residual stress formation, the analysis is continued with various thickness.

4.2 Analysis of the Residual Stresses due to Thickness of the Clad Material:

Analysis is carried out by varying the thickness of the clad layer. Initially 1mm thickness is considered to study the residual stress in the base structure.
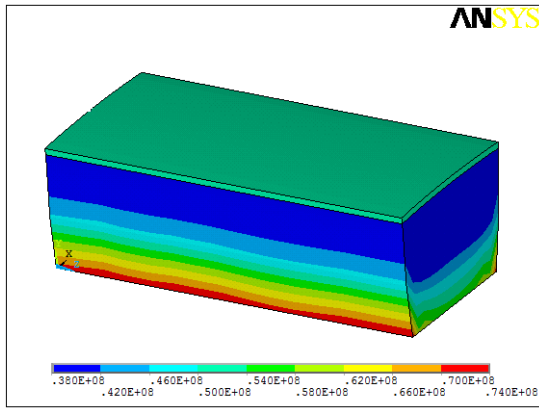
Fig. 4.20: Residual stress in the structure

Fig. 4.21: Residual stress due to 2mm thick clad material

The figure 4.20 shows residual stress formation of 74Mpa in the base material. This stress is less than 4mm clad thickness. This can be attributed to lesser temperature effect on the base structure.

The figure 4.21 shows residual stress formation of 78.2Mpa in the base material. This stress is less than 4mm clad thickness but higher than 1mm thick cladding. This can be attributed to higher thermal effect on the structure.

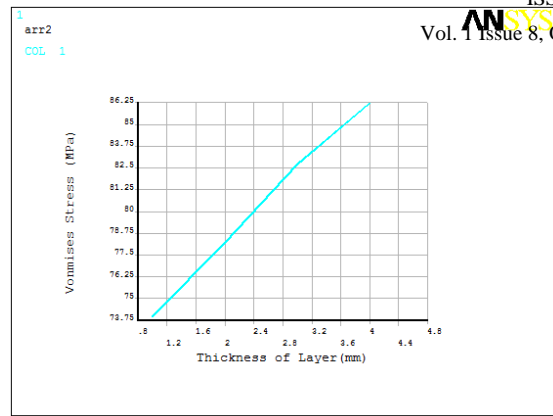**Fig. 4.22: Residual stress due to 3mm thick clad material**

Fig. 4.23: Thickness Vs Vonmises Stress with clad thickness

The figure 4.22 shows residual stress formation of 82.7Mpa in the base material. This stress is less than 4mm clad thickness but higher than 1mm and 2mm thick cladding. But the residual stress pattern is similar to the previous cases.
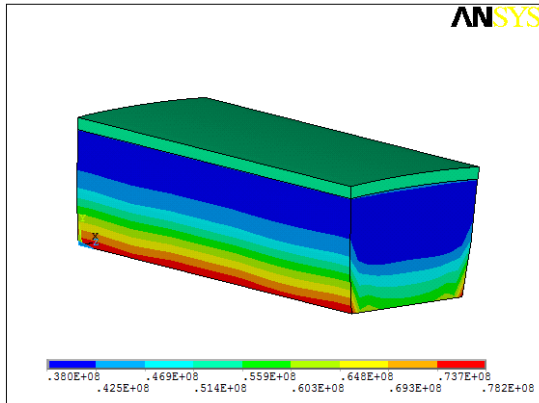
Table 4.1: Clad Thickness to Residual Stress formation

Clad Thickness	Vonmises Stress (Mpa)
1	74
2	78.2
3	82.7
4	86.2

The table 4.1 shows vonmises stress due to varying thickness of the clad material. The stress increasing with thickness of the clad material. Almost uniform increase of stress can be observed with clad thickness. This can be attributed higher heat content deposited in the process.

The figure 4.23 shows variation of vonmises stress with thickness of the clad material. The Vonmises stress is uniformly increasing with thickness. In the graph, the X-axis is represented with thickness of the clad material and Y-axis is represented with Vonmises with MPa. Further analysis is carried out with different materials to find best clad material. Aluminum brass and Zerconium is considered for comparision. The clad material properties are changed and analysis is carried out to find residual stress formation. The results are as follows.
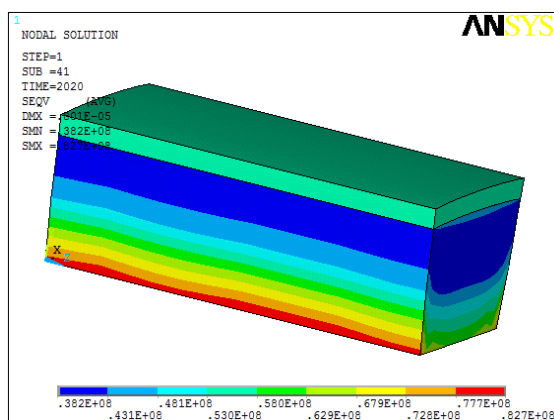
4.3   Analysis of the Residual Stresses with General Cladding Materials
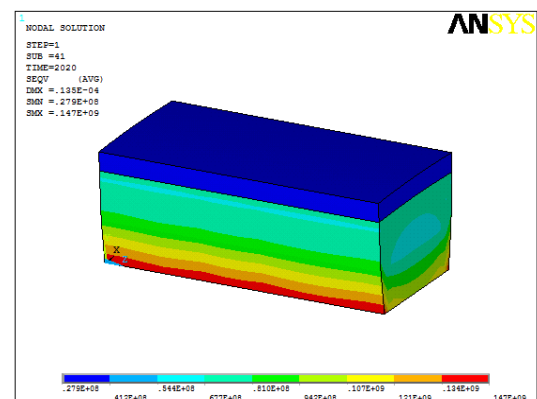
Fig. 4.24: Residual stress with Aluminum Cladding

Fig. 4.25: Vonmises stress plot

The figure 4.24 shows residual stress with aluminium cladding. Maximum stress is around 147Mpa. This stress more than the first case. This can be attributed to higher difference of thermal expansion coefficient of base metal and cladding material. Thermal strain is directly proportional to thermal expansion coefficient. Due to higher deformation of clad metal and lower expansion of base metal, the stresses will be more.

The figure 4.25 shows vonmises stress plot across the geometry. Minimum stress is observed on the aluminium material as the young's modulus is much smaller than the base metal modulus of rigidity.

Fig. 4.26: Residual stress with Brass Cladding

Fig. 4.27: Stress graph for Brass

The figure 4.26 shows residual stress with brass cladding. Maximum stress is around 130Mpa. This stress more than the first case. This can be attributed to higher difference of thermal expansion coefficient of base metal (11.7e-6) and cladding material (Brass -21e-6). Minimum stress is observed on the cladding material as the young's modulus of Brass (103GPa) is almost half of the parent metal (206GPa).

The figure 4.27 shows vonmises stress in the brass cladding. Again the stresses are less in Brass material compared to the base material. This is mainly due to higher young's modulus of steel compared to the brass. Also due to higher difference of thermal expansion coefficients, the stress generation is more in the structure.
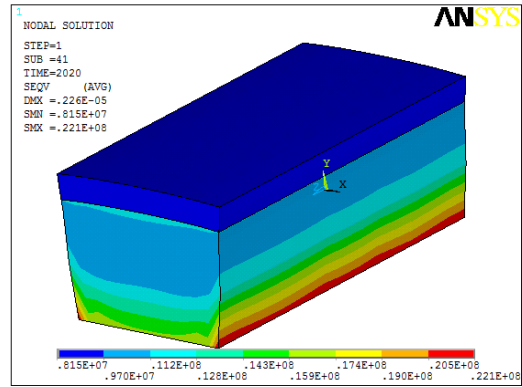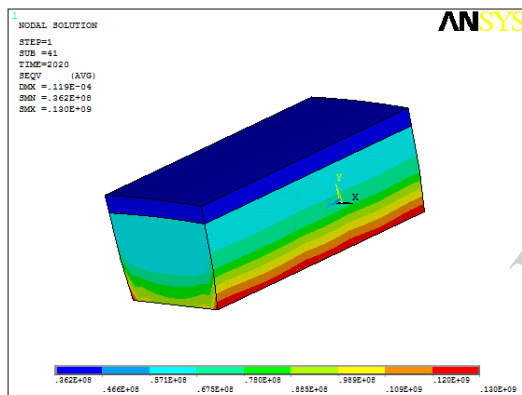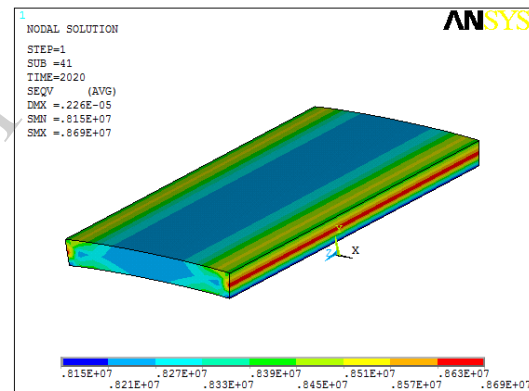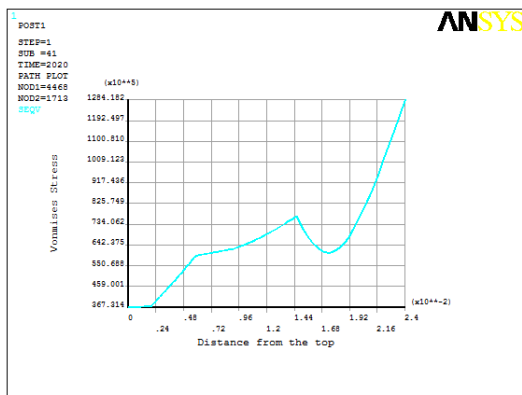
Zirconium cladding

Zirconium is the best material for the cladding as it comprises lowest thermal expansion coefficient compared to the most of the engineering materials with goo mechanical properties. The analysis is carried out by clad material properties to zirconium. The analysis results are as follows.

Fig. 4.28: Residual stress with Zirconium cladding

Fig. 4.29: Residual stress in the zirconium

The figure 4.28 shows residual stress formation with zirconium cladding. The least stress of 22.1Mpa can be observed with Zirconium material. The stress patterns are similar to the previous cases. But the stress generation is least with zirconium cladding for the base material. This is mainly attributed to the lowest coefficient of expansion of zirconium**.**

The figure 4.29 shows residual stress in the zirconium. The maximum stress of 8.69 Mpa can be observed in the material. This is the lowest thermal residual stress for the discussed materials. This results indicates lowest distortion in the material. The maximum stresses are observed at the central location shown with red colour.

Fig. 4.30: Graphical plot of Residual stress

The figure 4.30 shows residual stress in the structure with zirconium cladding. The maximum stress is observed in the base metal and minimum stresses on Zirconium. This is mainly due to difference in Young's modulus and thermal expansion coefficients.

Table 4.2: Residual stress generation in the base metal with different cladding materials

Material	Residual Stress(MPa)
Steel	86.2
Aluminium	147
Brass	130
Zirconium	22.1

The table shows residual stress formation with different cladding materials. Zirconium shows minimum residual stress in the structure. This can mainly attributed to lower thermal expansion coefficient due to heating which reduces the stresses in the structure.

4.4   Discussion:

In the present work cladding process is simulated using Finite element analysis using ANSYS. Initially clad geometry and base metal are modeled and split to ease map meshing. The meshed geometry is attributed with relevant properties. Initially the whole body is heated to 170 ^{0}c. Further analysis is carried out with cladding simulation block by block. The temperature plots are represented. The top clad geometry is subjected to higher temperature and the region away from cladding process is subjected to minimum temperature. The geometry is brought back to initial temperature by 2000 seconds cooling time. The analysis is converted to structural analysis by considering thermal loads to structural conditions. The coupled field analysis results represent a stress gradient with minimum stress on top and maximum stress in the constraint region indicates developed residual stress in the cladding process. The results show a stress development of 86.2 MPa in the structure. Further analysis is carried out to find the effect on thickness of cladding material on the residual stress formation. The analysis is carried out for 1mm, 2mm, 3mm and 4mm thickness. The results show lesser residual stress with lesser thickness of clad material. This may be attributed to lower heat input to the overall structure. Further analysis is carried out with different cladding materials. The results shows higher thermal expansion coefficient materials create higher stresses compared to the lower thermal expansion coefficient materials. The zirconium with its lower thermal expansion is the best engineering clad material with minimum residual stress formation in the structure. Also young's modulus plays important role in extent of stress in the materials.

5. Conclusions

5.1   Conclusions:

Thermal cladding process is simulated using Finite element software ANSYS. The temperature distribution in cladding process, usage of element birth and death, effect of clad material thickness and different clad materials in residual stress formation are obtained. The overall simulation is process as follows.

- Initially clad geometry along with base material geometry are built and split to ease brick meshing of the structure(Generally brick mesh gives better results compared to the free mesh)
- Initially thermal boundary conditions are applied with initial preheat temperature of 170 ^{0}c.The cladding process is simulated by element birth and death feature with Newton Raphson iterative technique.
- Temperature distribution and temperature variation across the section are plotted
- The members are cooled to initial temperature and residual estimations are carried out
- The coupled field analysis results show residual stress formation in the structure after cooling it to the room temperature. The maximum stresses are observed at the constraint region and less at the outer surface.
- Further analysis results are obtained by varying clad material thickness and results are obtained for residual stress formation. The results indicate lower residual stress with lesser thickness of the clad material. This may attributed to lower heat content due to lesser thickness of the clad material.
- Further analysis is carried out with general clad materials. The results are obtained for residual stresses for all the materials. The results shows zirconium is the best cladding material with lowest residual stresses in the structure. The results also prove that thermal expansion coefficient and Young's modulus plays important role in the residual stress formation.
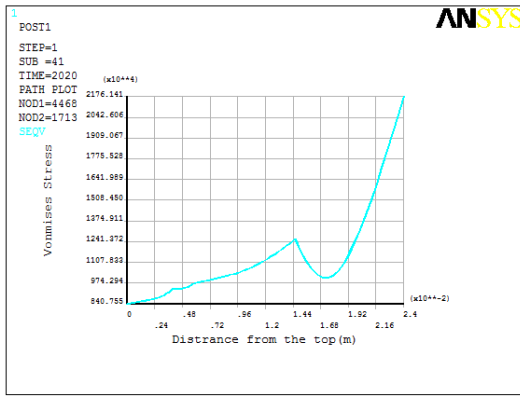
References

[1]   Heyn, E. and Bauer, "Measurement of Residual Stresses in Cold Drawn Metals." *Internationale Zeitschrift fur Met alio graphie,* Vol.1, pp. 16-50.1911

[2]   Mesnager, M. "Methods de Determination des tensions existant dans unCylindre Circulare." *Compt. Rend.,* Vol. 169, pp. 1391-1393.1919

[3]   Sachs, G. Z. "Evidence of Residual Stresses in Rod and Tubes." *Trans. ASME,* Vol. 19, pp. 352-357.1927

[4]   Hayes, Thomas, J. *Elements of Ordinance.* John Wiley & Sons, N.Y.1938

[5]   *Timoshenko*, S., Theory of Elasticity, McGraw-Hill Book Co.,. Inc., New ...1941

[6]   A. *Robertson*. ... Contractions and Stresses in Butt Welded Steel Plates (London, H.M.S.O., *1950.*

[7]   Demorest, D. J. *A Study of Residual Stresses in Flat Beams by Electropolishing Methods,* Ohio State University, OH.1950

[8]   Horger, O. J. *Residual Stresses • Handbook of Experimental Stress Analysis,* Edited by M. Hetenyi. John Wiley & Sons, N.Y.1950

[9]   Leeser, D. O. and Daane, R. A. "Experimental Stress Analysis." Argonne National Laboratory, Lemont, IL. pp. 203-208.1953.

[10]   Dieter Jr. G. E.: *Mechanical Metallurgy*. McGraw-Hill, p395, 1961.

[11]   I. J. Kumar and D. Rajgopalan, "*Thermal stresses in hollow cylinder due to a sinusoidal surface*

heating source", Defense Science Laboratory, Delhi, 1969, Volume 1(3), Pages 305 -319.

[12] R. Srinivasan, C.S. Hartley and R. Bandy, "Residual Stress Determination in Inconel-600 Tubes Using Electro-Chemical Machining," in Novel Techniques in Metal Deformation Testing, R.H. Wagoner, Editor, TMS/AIME, Warrendale, Pennsylvania, pp 163-174 1983.

[13] J. *Rasty*, "Effect of Combined Corrosion and *Residual Stress* on ..... Research and Development Center, United Technologies, July 11-12, *1987*,

[14] Rasty, J. and Hartley, C. S.. *Experimental Measurement of Residual Stresses in Nuclear Fuel Cladding,* Louisiana State University, Baton Rouge, 1987

[15] P. Dupas and D. Moinereau, "**Evaluation of Cladding Residual Stresses in Clad Blocks by Measurements and Numerical Simulations"** JOURNAL DE PHYSIQUE IV Colloque C1, supplement au Journal de Physique 111, Volume 6, Javier 1996.

[16] Rolf Paschold, ESAB GmbH Solingen, "Submerged Arc strip cladding of continuous casting rollers using OK band 11.82 and OK flux 10.07, Svetsaren Nr 1., 17-19, 2001.

[17] G. Sánchez Sarmiento, M.J. Mizdrahi, P. Bastias, M. Pizzi, "*Heat Transfer Thermal-Stress and Pipe-whip Analysis in Steel Pipes of a Nuclear Power plant*", ABAQUS Users' Conference, Pages 631 – 645, 2004.

[18] Muhammad Abid, "*Determination of safe operating conditions for gasketed flange joint under combined internal pressure and temperature: A finite element approach*", International Journal of Pressure Vessels and Piping volume 83, Pages 433–441, January 2006.

[19] Iradj Sattari – Far, Magnus Andersson, "Cladding Effects on Structural Integrity of Nuclear Components", Inspecta Technology AB. June 2006.

[20] Murali Krishna M, Shunmugam M.S., Siva Prasad N, "*A study on the sealing performance of bolted flange joints with gaskets using finite element analysis*", International Journal of Pressure Vessels and Piping, Volume 84, February 2007, Pages 349–357, February 2007.

[21] Mohammad A. Irfan, Walter Chapman, "*Thermal stresses in radiant tubes due to axial, circumferential and radial temperature distributions*", Applied Thermal Engineering, page 1913-1920, Volume 29, September 2008,

[22] ANSYS analysis user's manual, Version 10, theory reference.

[23] Lochan Sharma, "Development of Submerged arc welding fluxes for enhanced corrosion resistance of structural steel welds".

[24] "Technical handbook strip cladding", ESAB AB.